MODIFIED GAUSSIAN NOISE DE-NOISING USING ORTHONORMAL WAVELETS

[1]**Anamika Jain**
Research Scholar,
Dept. of ECE, SRIT, Jabalpur

[2] **Divyanshu Rao**
Assistant Professor,
Dept. of ECE, SRIT, Jabalpur

[3] **Prof. Ravimohan**
HOD, M.Tech.
Dept. of ECE, SRIT, Jabalpur

ABSTRACT: ***In this work, investigation of several well-known algorithms for image denoising is carried out & their performances with their methodologies are comparatively assessed. A new algorithm based on the orthonormal wavelet transform (OWT) is developed. This shows better performance in comparison with the performance of other algorithms. In addition, it has been shown to enjoy the advantage of implementation simplicity. There are different types of noises that may corrupt an image in real life such as, salt-pepper noise, Sparkle noise shot noise, amplification noise, quantization noise etc. However, AWGN or Gaussian noise was considered in this work. A major part of the work was devoted to the review, implementation & performance assessment of published image denoising algorithms based on various techniques including the wavelet transform. The wavelet based approach finds applications in denoising images corrupted with Gaussian noise. The well-known Lena image corrupted with AWGN was denoised using OWT wavelet methods.***

KEYWORDS: AWGN, Image Denoising, Noise, DWT, OWT.

I. INTRODUCTION

Image denoising is often used in the field of photography or publishing where an image was somehow degraded but needed to be improved before it can be printed. For this type of application we need to know something about the degradation process in order to develop a model for it. When we have a model for the degradation process, the inverse process can be applied to the image to restore it back to the original form. This type of image restoration is often used in space exploration to help eliminate artifacts generated by mechanical jitter in a spacecraft or to compensate for distortion in the optical system of a telescope [4]. Image denoising finds applications in fields such as astronomy where the resolution limitations are severe, in medical imaging where the physical requirements for high quality imaging are needed for analyzing images of unique events, and in forensic science where potentially useful photographic evidence is sometimes of extremely bad quality. Let us now consider the representation of a digital image. A 2-dimensional digital image can be represented as a 2-dimensional array of data $s(x,y)$, where (x,y) represent the pixel location. The pixel value corresponds to the brightness of the image at location (x,y). Some of the most frequently used image types are binary, gray-scale and color. Binary images are the simplest type of images and can take only two discrete values, black and white. Black is represented with the value „0" while white with „1". Note that a binary image is generally created from a gray-scale image. A binary image finds applications in computer vision areas where the general shape or outline information of the image is needed. They are also referred to as 1 bit/pixel images [5].Gray-scale images are known as monochrome or one-color images. The images used for experimentation purposes in this thesis are all gray-scale images. They contain no color information. They represent the brightness of the image. This image contains 8 bits/pixel data, which means it can have up to 256 (0-255) different brightness levels.

A „0" represents black and „255" denotes white. In between values from 1 to 254 represent the different gray levels. As they contain the intensity information, they are also referred to as intensity images. Color images are considered as three band monochrome images, where each band is of a different color. Each band provides the brightness information of the corresponding spectral band. Typical color images are red, green and blue images and are also referred to as RGB images. This is a 24 bits/pixel image.

II. DISCRETE WAVELET TRANSFORM (DWT)

Wavelets are mathematical functions that analyze data according to scale or Resolution. They aid in studying a signal in different windows or at different resolutions. For instance, if the signal is viewed in a large window, gross features can be noticed, but if viewed in a small window, only small features can be noticed. Wavelets provide some advantages over Fourier transforms. For example, they do a good job in approximating signals with sharp spikes or signals having discontinuities. Wavelets can also model speech, music, video and non-stationary stochastic signals. Wavelets can be used in applications such as image compression, turbulence, human vision, radar, earthquake prediction, etc. The term "wavelets" is used to refer to a set of Ortho-normal basis functions generated by dilation and translation of scaling function φ and a mother wavelet ψ. The finite scale multi resolution representation of a discrete function can be called as a discrete wavelet transform. DWT is a fast linear operation on a data vector, whose length is an integer power of 2. This transform is invertible and orthogonal, where the inverse transform expressed as a matrix is the transpose of the transform matrix. The wavelet basis or function, unlike sine and cosines as in Fourier transform, is quite localized in space. But similar to sine and cosines, individual wavelet functions are localized in frequency. The Ortho-normal basis or wavelet basis is defined as:

$$\varphi_{(j,k)}(x) = 2^{\frac{j}{2}}\varphi(2^j x - k)$$

The scaling function is given as:

$$\emptyset_{(j,k)}(x) = 2^{\frac{j}{2}}\varphi(2^j x - k)$$

Where ψ is called the wavelet function and j and k are integers that scale and dilate the wavelet function. The factor „j" is known as the scale index, which indicates the wavelet"s width. The location index k provides the position. The wavelet function is dilated by powers of two and is translated by the integer k. In terms of the wavelet coefficients, the wavelet equation is

$$\varphi(x) = \sum_{k}^{N-1} gk\sqrt{2}\emptyset(2x - k)$$

Where, g0, g1, g2. are high pass wavelet coefficients. Writing the scaling equation in terms of the scaling coefficients as given below, we get

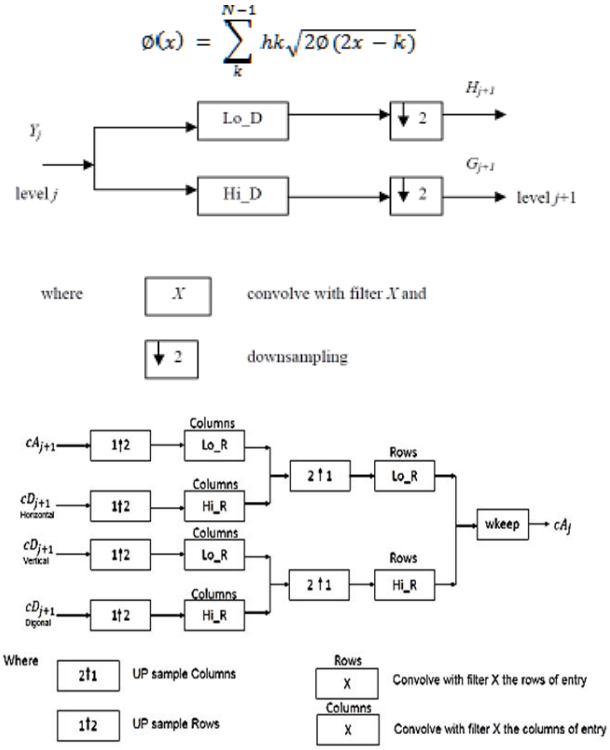

Figure 1: A 1-Dimensional DWT - Decomposition step

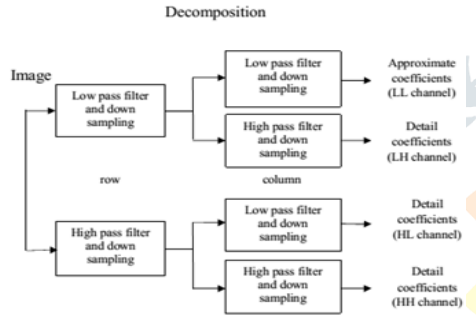

Figure 2: One level wavelet decomposition of two dimensional data

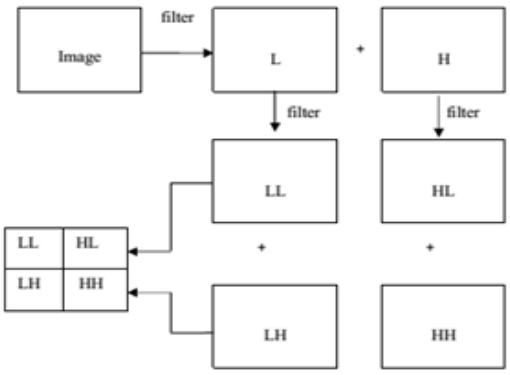

Figure 3: Subbands in wavelet decomposition of two dimensional data

DWT is the multi resolution description of an image. The decoding can be processed sequentially from a low resolution to the higher resolution. DWT splits the signal into high and low frequency parts. The high frequency part contains information about the edge components, while the low frequency part is split again into high and low frequency parts. The high frequency components are usually used for watermarking since the human eye is less sensitive to changes in edges. In two dimensional applications, for each level of decomposition, we first perform the DWT in the vertical direction, followed by the DWT in the horizontal direction. After the first level of decomposition, there are 4 sub-bands: LL1, LH1, HL1, and HH1. For each successive level of decomposition, the LL Sub-band of the previous level is used as the input. To perform second level decomposition, the DWT is applied to LL1 band which decomposes the LL1 band into the four sub- bands LL2, LH2, HL2, and HH2.

To perform third level decomposition, the DWT is applied to LL2 band which decompose this band into the four sub-bands – LL3, LH3, HL3, HH3. This results in 10 sub-bands per component. LH1, HL1, and HH1 contain the highest frequency bands present in the image tile, while LL3 contains the lowest frequency band.

DWT is currently used in a wide variety of signal processing applications, such as in audio and video compression, removal of noise in audio, and the simulation of wireless antenna distribution.

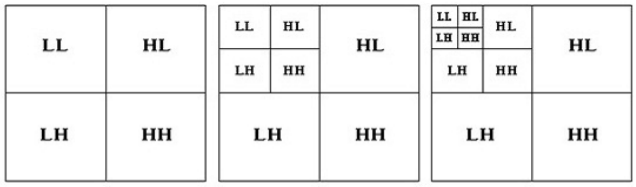

Figure 4: 3 level discrete wavelet decomposition

Wavelets have their energy concentrated in time and are well suited for the analysis of transient, time-varying signals. Since most of the real life signals encountered are time varying in nature, the Wavelet Transform suits many applications very well. As mentioned earlier, the wavelet equation produces different wavelet families like Daubechies, Haar, Coiflets, etc. The filter lengths and the number of vanishing moments for four different wavelet families are tabulated in Table 1.

Wavelet Family	Filters length	Number of vanishing moments, N
Haar	2	1
Daubechies M	$2M$	M
Coiflets M	$6M$	$2M$-1
Symlets	$2M$	M

Table 1: Wavelet families and their properties

The term wavelet thresholding is explained as decomposition of the data or the image into wavelet coefficients, comparing the detail coefficients with a given threshold value, and shrinking these coefficients close to zero to take away the effect of noise in the data. The image is reconstructed from the modified coefficients. This process is also known as the inverse discrete wavelet transform. During thresholding, a wavelet coefficient is compared with a given threshold and is set to zero if its magnitude is less than the threshold; otherwise, it is retained or modified depending on the threshold rule. Thresholding distinguishes between the coefficients due to noise and the ones consisting of important signal information.

Wavelet Denoising

There are many techniques for image denoising which are using wavelet & based on wavelet shrinkage & wavelet thresholding. The computational advantage of using such estimation approaches is provided by algorithms of fast implementation. The smaller coefficients are instead eliminated, hence sparsifying the wavelet expansion. The simplest model of Image Degradation/Restoration Process:

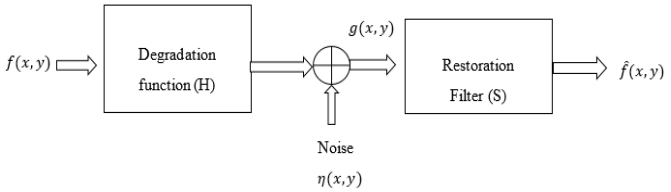

Figure 5: Model of the image degradation/restoration process

Wavelets provide a good expansion basis for the unknown function, because it can satisfy both parsimony & sparsity properties simultaneously; while the latter comes front the inherent distribution of the "energy" of the function over the coefficient vector, hence naturally selecting a subset of them as the most significant. This thesis work involves the denoising of intensity images with formats like JPG. Bto.1P. PNG & TIF [7].

One of the most important properties of wavelets is that they provides unconditional bases for many other different signal classes. Hence, most of the signal information in wavelet expansions is conveyed by a relatively small number of large coefficients. The process of denoising using wavelets has been described by [14] & called "Wavelet Shrinkage". In many systems, the concept of additive white Gaussian noise (AWGN) is used. This simply means a noise, which has a Gaussian probability density function & white power spectral density function (noise distributed over the entire frequency spectrum) & is linearly added to whatever signal used for analyzing.

This work focuses primarily on thresholding as a means of denoising in the wavelet-domain due to some important characteristics present in wavelet coefficients.

The noisy input signal can be thought of as the sum of the desired signal component (or true signal) & the additive white Gaussian noise (AWGN) with variance of σ^2 & is shown in equation below.

$$S(x,y) = f(x,y) + \sigma^2\, n(x,y)$$

Where; f (x,y) is desired signal & n (x,y) is noisy component. It has been shown that when the wavelet basis selected, matches well with the signal characteristics, a very few of the wavelet detail coefficients are influenced by the signal, while most of them are influenced by the noise. Therefore, an expression for the wavelet coefficients at each decomposition level can be described by the equation 3.3:

$$y_j(i) = w_j(i) + n_j(i) \qquad \ldots\ldots\ldots (3.3)$$

In addition, the desired signal coefficients are expected to be of larger magnitude when the SNR is not too small. Therefore, denoising is accomplished by thresholding wavelet coefficients, thereby eliminating noise-only coefficients & keeping the desired signal coefficients for reconstruction.

III. PROPOSED METHODOLOGY

This section contains the stepwise, detailed methodology that is followed while denoising images using Orthonormal wavelets basis with eight vanishing moments (sym8) over four decomposition stages. The wavelet coefficients that lie on the same dyadic tree, are well known to be large together in the neighborhood of image discontinuities. What can, thus, be predicted with reasonably good accuracy are the position of large wavelet coefficients out of parents at lower resolutions. However, getting the actual values of the finer resolution scale coefficients seem somewhat out of reach. This suggests that the best we can get out of between-scale correlations is a segmentation between regions of large and small coefficients. In a critically sampled orthonormal wavelet decomposition, the parent subband is half the size of the child subband. The usual way of putting the two subbands in correspondence is simply to expand the parent by a factor two. Unfortunately, this approach does not take into account the potential non-integer shift caused by the filters of the DWT. We, thus, propose a more sophisticated solution, which addresses this issue and ensures the alignment of image features between the child and its parent. This idea comes from the following observation: Let LH_j and LL_j be, respectively, band pass and low pass outputs at iteration of the filter bank. Then, if the group delay between the bandpass and the low pass filters are equal, no shift between the features of Let LH_j and LL_j will occur. Of course, depending on the amplitude response of the filters, some features may be attenuated, blurred, or enhanced, but their location will remain unchanged. When the group delays differ, which is the general case, we, thus, propose to filter the low pass subband LL_j in order to compensate for the group delay difference with LH_j. LL_j is filtered in the three bandpass "directions" by adequately designed filters W_{HL}, W_{HH} & W_{LH} providing aligned, i.e., group delay compensated, subbands with HL_j, HH_j & LH_j.

For better & easy understanding, a complete flowchart of the discussed methodology has been shown at the end of this chapter. The proposed algorithm steps are as follows:

Step 1:
Read the test image (original).

Step 2:
Resize the test image & convert it into Gray scale image. The images taken for rectification have a lot of variation in their sizes & hence cannot be compared on the same basis. For large sized images, such as 1024×1024, the computation time for denoising is found to be more difficult & if the image size is taken smaller.

Step 3:
Noise is added to the standard test images. In this work AWGN is added for generation of noisy image. The gaussian noise adds normal distributed noise to the original image. Main feature of this noise, it is independent of the image on which it is going to be applied. The pixel value altered by the additive Gaussian noise can be shown as:

$$J(k,l) = x(k,l) + n$$

Where n is the noise, $n \sim N(0, v)$, being distributed normally with variance v.

Step 4:
Make the noisy image to undergo Orthonormal wavelet transform, OWT. A well-known orthogonal basis expansion is obtained by discrete wavelet transform WT^d, by which a map $f \to w$ is implemented via a bank of quadrature mirror filters by $w = W^d f$ & co-efficient at high/low scale (with high & low frequency content, respectively) are obtained. For an orthogonal wavelet basis is used, such as db, Symlets or coiflet, then;

$$y = f + \xi$$

Become transformed in:

$$W^d y = W^d f + W^d \xi \equiv g + \eta$$

This transformation preserves Gaussianity (as from the noise ξ) & produces decorrelation for auto-correlated systems.

Step 5:
After the noisy image is decomposed into approximation & detail coefficients using wavelet transform, it is made to undergo the following thresholding rules having various threshold values. In addition, two cases have been considered- one where the low pass components are not thresholded & the other being the one where the low pass components have been thresholded. The thresholding techniques applied are as follows,

- Soft thresholding- Refers to the procedure where firstly the input elements with absolute value lower than the defined threshold value, are set to zero & are then scaled to the non-zero coefficients toward zero. It eliminates discontinuity & gives more visually pleasant images.

$$x = abs(y)$$

$$x = sign(y).*(x \geq thld).*(x - thld)$$

Where y is the input, thld is the threshold value & x is the thresholded output.

- Hard thresholding- refers to the procedure where the input elements with absolute value lower than the defined threshold value, are set to zero. It is discontinuous at the point where $|x| = thld$ & yields abrupt artifacts in the recovered images especially when the noise energy is significant.

$$x = (abs(y) > thld).*y$$

Step 6:

After the decomposed image coefficients are thresholded using the above mentioned three threshold values with each of the thresholding technique, the denoised image is reconstructed using inverse Orthonormal wavelet transform.

Step 7:

PSNR is calculated for all the standard images with their noisy & denoised image counterparts, respectively.

- PSNR- PSNR stands for the peak signal to noise ratio. It is a term used to calculate the ratio of the maximum power of a test signal & the power of noise corrupted version of the test signal. It is calculated as the following:

$$MSE = \frac{1}{mn}\sum_{i=0}^{m-1}\sum_{j=0}^{n-1}\|I(i,j) - K(i,j)\|^2$$

$$PSNR = 10.*log_{10}\left(\frac{MSE_i^2}{MSE}\right)$$

Where I & K are the original & noisy / denoised image, respectively. MAX_I is the maximum pixel value of the image under test. For an image having 8 bits per sample, pixels representation, this is equivalent to $2^8 = 255$.

At one time, we calculate PSNR for original with noisy image & refer it as PSNR (O/N). After the image is denoised, it is calculated for original with denoised image & is then referred as PSNR (O/D). Hence, it shows the improvement in the noisy image after denoising, if any. Flow chart of the proposed algorithm is shown in figure 6;

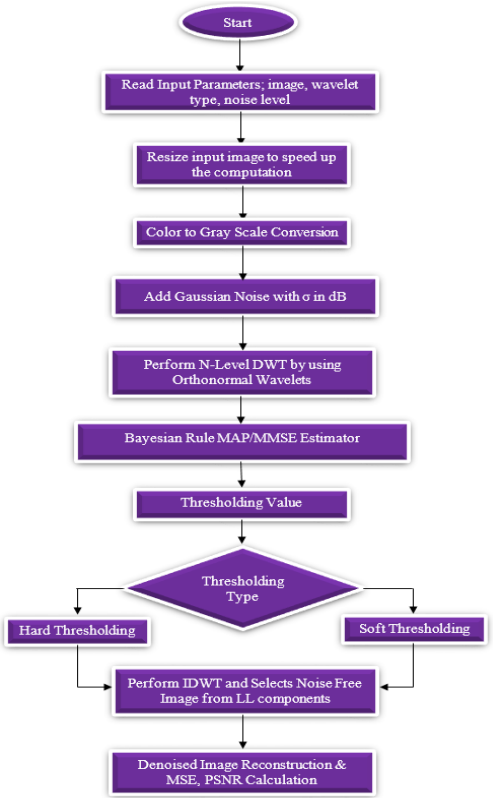

Figure 6: Flowchart of Proposed Image Denoising Algorithm

IV. SIMULATION RESULTS & DISCUSSIONS

In simulation we have done the simulations with Orthonormal wavelets basis with eight vanishing moments (sym8) over four decomposition stages.

IV.1 Test Image Lena & Proposed Denoising Method

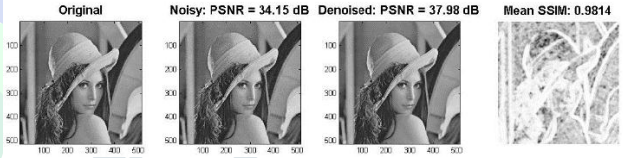

Figure 7: Simulation results for test image 'Lena' proposed method using 'Symlet' wavelet at 5 dB AWGN noise

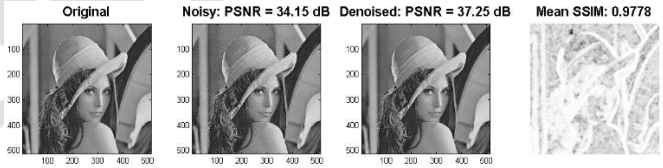

Figure 8: Simulation results for test image 'Lena' proposed method using 'Haar' wavelet at 5 dB AWGN noise

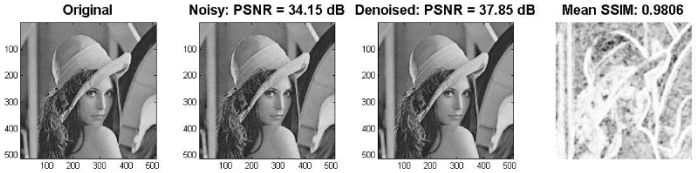

Figure 9: Simulation results for test image 'Lena' proposed method using 'Daubechies' wavelet at 5 dB AWGN noise

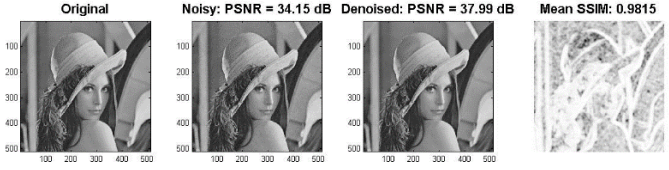

Figure 10: Simulation results for test image 'Lena' proposed method using 'Coiflets' wavelet at 5 dB AWGN noise

Figure 7-10 shows the simulation results of test image 'Lena' taken for simulation of our proposed algorithms by using distinguish wavelets. Simulation results values of PSNR & MSE for different wavelets are tabulated in table 6.1.

IV.2 Simulation Results Table of Proposed Work (Lena.jpg)

Noise Variance	Noisy Image Parameters	
σ	PSNR (dB)	MSE
5	34.1550	24.9793
10	28.1381	99.8314
15	24.5817	226.4202
20	22.1175	399.3256
25	20.1721	624.9882
30	18.6068	900.00

Table 2: Noisy image parameters

Noise Variance	Using Haar Wavelet			Using Symlet Wavelet			Using Daubechies Wavelet			Using Coiflet Wavelet		
σ	PSNR (dB)	MSE	SSIM	PSNR (dB)	MSE	SSIM	PSNR (dB)	MSE	SSIM	PSNR (dB)	MSE	SSIM
5	37.25	12.24	0.9778	37.98	10.36	0.9814	37.85	10.66	0.9806	37.99	10.33	0.9815
10	33.51	28.99	0.9474	34.57	22.70	0.9586	34.28	24.29	0.9548	34.58	22.63	0.9588
15	31.49	46.29	0.9176	32.69	35.03	0.9367	32.29	38.39	0.9286	32.70	34.93	0.9368
20	30.12	63.21	0.8894	31.38	47.36	0.9158	30.92	52.64	0.9028	31.39	47.24	0.9157
25	29.09	80.17	0.8626	30.37	59.67	0.8957	29.88	66.79	0.8783	30.38	59.55	0.8956
30	28.28	96.65	0.8376	29.56	71.91	0.8769	29.06	80.68	0.8553	29.57	71.78	0.8767

Table 3: Test Image Lena Simulation Results

Table 3 shows that proposed method using distinguish wavelets for different values of noise variance in dB. Also we can see from the table that with Coiflet Wavelet performs better than Symlet, Haar & Daubechies wavelets. The proposed Orthonormal wavelet transform (OWT) method has minimum Mean Square & highest PSNR with Haar wavelets.

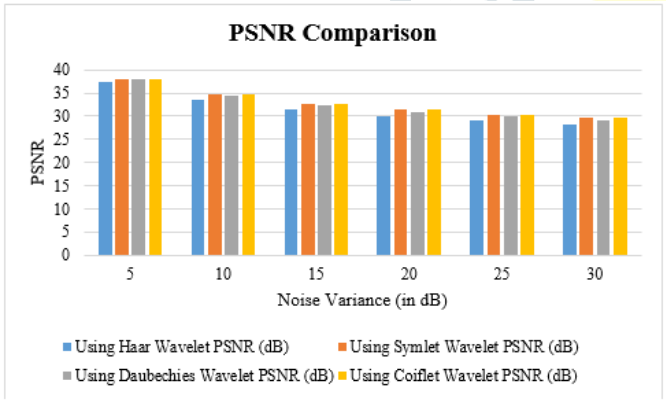

Figure 11: PSNR vs Noise Variance graph for test image 'Lena'

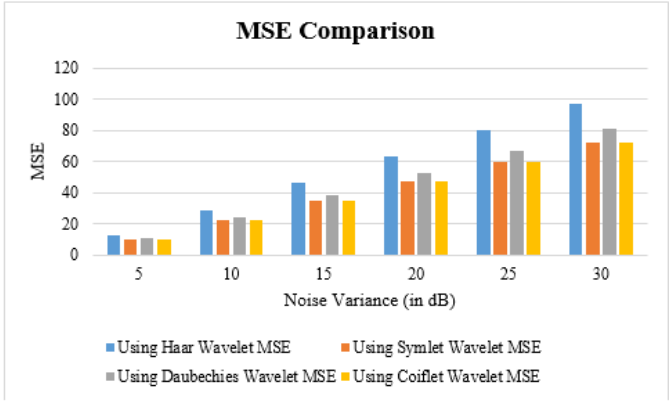

Figure 12: MSE vs Noise Variance graph for test image 'Lena'

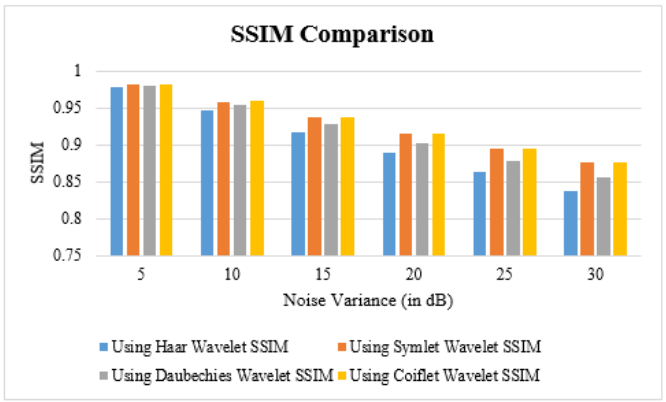

Figure 13: SSIM vs Noise Variance graph for test image 'Lena'

IV.3 Simulation Results Comparison Table (Lena Image)

Noise Variance σ / Algorithm	σ =10	σ =20	σ =30
Proposed Work (Coiflets)	34.58	31.39	29.67
CD-B-k D [1]	33.95	31.35	29.55
HMT [2]	33.81	30.36	28.45
NIG-NSCT [4]	33.74	31.18	29.09
NIG-WT [4]	31.97	28.42	26.27
Bayes-Shrink [2]	33.29	30.14	28.26
NIG-CT [6]	33.32	31.06	29.33
AS-CT [9]	33.77	31.48	29.64
Visu-shrink [11]	30.65	27.76	26.33

Table 4: Test Image Lena Simulation Results Comparison

Table 4 shows that proposed method with Coiflet Wavelet gives better results as compared to other existing methods mentioned in literature for different values of noise variance for 10 dB, 20 dB & 30 dB. We have taken Lena image for comparison. The proposed method has minimum Mean Square & highest PSNR with Haar wavelets. The proposed has 0.63 dB improvement for σ =10 dB, 0.04 dB improvement for σ =20 dB & 0.12 dB improvement for σ =30 dB as compared to Contourlet Domain Image Denoising based on the Bessel k-form Distribution (CD-B-k D) [1].

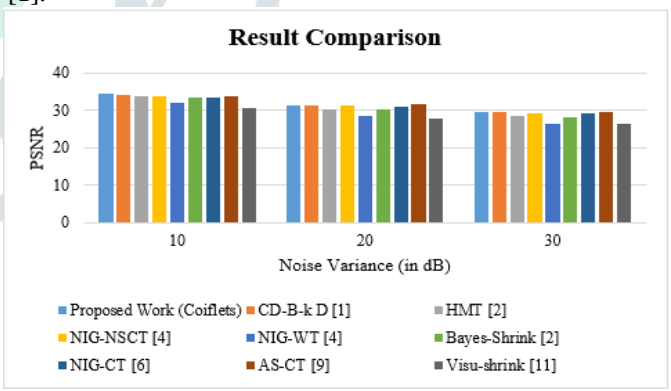

Figure 14: PSNR comparison graph for test image 'Lena'

V. CONCLUSION

In this paper image denoising techniques for the AWGN corrupted has been given. A new algorithm based on the orthonormal wavelet transform (OWT) is developed. This shows better performance in comparison with the performance of other algorithms. In addition, it has been shown to enjoy the advantage of implementation simplicity. There are different types of noises that may corrupt an image in real life such as, salt-pepper noise, Sparkle noise shot noise, amplification noise, quantization noise etc. However, AWGN or Gaussian noise was considered in this work. A major part of the work was devoted to the review, implementation & performance assessment of published image denoising algorithms based on various techniques including the wavelet transform. The wavelet based approach finds applications in denoising images

corrupted with Gaussian noise. The well-known Lena image corrupted with AWGN was denoised using OWT wavelet methods. Simulation results prove that; our proposed algorithm is better with previous works on image denoising.

REFERENCES

[1] H. Sadreazami et-al, "Contourlet Domain Image Denoising based on the Bessel k-form Distribution", IEEE 28th Canadian Conference on Electrical and Computer Engineering Halifax, Canada, May 3-6, 2015.

[2] Liqiang Shi, "An Improved Image Denoising Algorithm", Seventh IEEE International Conference on Measuring Technology and Mechatronics Automation, 2015.

[3] Cuong Cao Pham et-al, "Efficient image sharpening and denoising using adaptive guided image filtering", Published in IEEE, IET Image Processing Magazine, Pp. 71 – 79, 2015.

[4] Wangmeng Zuo et-al, "Gradient Histogram Estimation and Preservation for Texture Enhanced Image Denoising", IEEE Transactions on Image Processing, Volume 23, Nn. 6, JUNE 2014.

[5] Vikas Gupta et-al, "Image Denoising using Wavelet Transform method", Tenth IEEE International Conference on Wireless and Optical Communications Networks (WOCN), Pp 1-4, 2013.

[6] Fuqing Jia et-al, "Image Denoising Using Hyper-Laplacian Priors and Gradient Histogram Preservation Model", 12th IEEE International Conference on Signal Processing (ICSP), 2014.

[7] Ajay Boyat et-al, "Image Denoising using Wavelet Transform and Median Filtering", Nirma University IEEE International Conference on Engineering (NUiCONE), 2013.

[8] Paras Jain & Vipin Tyagi, "Spatial and frequency domain filters for restoration of noisy images", IETE Journal of Education, 54(2), 108-116, 2013.

[9] Maggioni, M., Katkovnik, V., Egiazarian, K., Foi, "A.: Nonlocal transform-domain filter for volumetric data denoising and reconstruction", IEEE Transaction on Image Processing, 22(1), 119–133, 2013.

[10] Silva, R.D., Minetto, R., Schwartz, W.R., Pedrini, H.: Adaptive edge-preserving image denoising using wavelet transforms. Pattern Analysis and Applications. Springer, Berlin doi:10.1007/s10044-012-0266-x, 2012.

[11] Zhang, Y., Li, C., Jia, J, "Image denoising using an improved bivariate threshold function in tetrolet domain", 2013.

[12] Dai, L., Zhang, Y., Li, Y.: Image denoising using BM3D combining tetrolet prefiltering. Inf. Technol. J. 12(10), 1995–2001, 2013.

[13] He, K., Sun, J., Tang, X.: Guided image filtering. In: Proceedings European Conference on Computer Vision, pp. 1–14, 2010.

[14] Porikli, F, "Constant time O(1) bilateral filtering", In Proceeding IEEE Conference on Computer Vision and Pattern Recognition, Anchorage, pp. 1–8, 2008.

[15] Yang, Q., Tan, K.H., Ahuja, N, "Real-time O(1) bilateral filtering", In Proceedings IEEE Conference on Computer Vision and Pattern Recognition, Miami, pp. 557–564, 2009.

[16] Farbman, Z., Fattal, R., Lischinski, D., Szeliski, "R.: Edge-preserving decompositions for multi-scale tone and detail manipulation", ACM Transactions on Graphics 27(3), 1–10, 2008.

[17] Paris, S., Durand, F, "A fast approximation of the bilateral filter using signal processing approach", In the Proceeding of European Conference on Computer Vision, pp. 568–580, 2006.

[18] Gonzalez, R.C., Woods, R.E.: Digital image processing, 3rd edn. Prentice-Hall, Upper Saddle River, 2008.

[19] Blu, T., Luisier, F, "The SURE-LET approach to image denoising", IEEE Transaction Image Processing, 16(11), 2778–2786, 2007.

[20] Paris, S., Durand, F.: A fast approximation of the bilateral filter using signal processing approach. In: Proceeding European Conference on Computer Vision, pp. 568–580, 2006.

[21] Dabov, K., Foi, A., Katkovnik, V., Egiazarian, K.: Image denoising with block-matching and 3D filtering. In: SPIE electronic imaging: algorithms and systems, vol. 6064, pp. 606414-1–606414-12, 2006.

[22] Yuan, X., Buckles, B.: Subband noise estimation for adaptive wavelet shrinkage. In: Proceeding 17th International Conference on Pattern Recognition, vol. 4, pp 885–888, 2004.

[23] Elad, M.: On the origin of the bilateral filter and ways to improve it. IEEE Transaction Image Processing, 11(10), 1141–1151, 2002.

[24] Sendur, L., Selesnick, I.W.: Bivariate shrinkage functions for wavelet-based denoising exploiting interscale dependency. IEEE Trans. Signal Process. 50(11), 2744–2756, 2002.

[25] Chang, S., Yu, B., Vetterli, M.: Spatially adaptive wavelet thresholding based on context modeling for image denoising. IEEE Trans. Image Process. 9(9), 1522–1531, 2000.